20% Efficient Screen-Printed Cells With Spin-On-Dielectric-Passivated Boron Back-Surface Field

Arnab Das, Vichai Meemongkolkiat, Dong Seop Kim, Saptharishi Ramanathan, and Ajeet Rohatgi, *Fellow, IEEE*

***Abstract*—This paper reports on the characteristics of a spin-on dielectric which has been used as the rear-surface passivation layer to achieve 20% efficient screen-printed (SP) boron back-surface field (B-BSF) solar cells. The dielectric provides, in a single thermal step, both stable passivation of a heavily doped p^+ surface and strong gettering of iron which is a common contaminant in high-temperature boron diffusion processes. It was found that gettering of silicon substrates, contaminated during boron diffusion, is most effective when the dielectric is deposited on top of the boron-doped layer. The effect of dielectric charge density on passivation of p^+ surfaces was also studied and a very high charge density of -10^{13} cm^{-2} was found to be necessary to significantly improve the passivation on surfaces with a boron concentration $> 10^{19}$ cm^{-3}.**

***Index Terms*—Boron, charge carrier lifetime, dielectric films, gettering, passivation, photovoltaic cells, surface charging.**

I. Introduction

DUE to the high cost of silicon, both high-efficiency and thinner substrates are key to achieving grid parity with silicon photovoltaics. From cost modeling roadmaps, it was found that ~20% efficient screen-printed (SP) cells at a price of ~$1.25/W can get us close to grid parity. However, the dominant SP aluminum back-surface field (Al-BSF) technology appears to be insufficient for reaching this target as production cell efficiencies achieved on this structure are only in the range of 17%–19% on ~200 μm thick substrates [1]. Therefore, there is a need for higher efficiency cell structures. This paper shows that 20% efficient SP cells can be achieved using a passivated boron back-surface field (B-BSF) structure. In a previous paper, we introduced a novel spin-on dielectric which can passivate a B-BSF and getter lifetime-reducing contamination that is common in boron diffusions [2]. This paper expands on those results by quantifying improvements to the rear side of the cell that would allow efficiency to increase from 19% to 20% and discusses the tradeoffs associated with the various processes that fulfill those requirements. In addition, we have used PC1D modeling to quantify the impact of negatively charged dielectrics on BSF cells and the tradeoffs associated with using processes that benefit most from such dielectrics [3].

Manuscript received January 6, 2010; revised June 9, 2010; accepted June 23, 2010. Date of publication August 16, 2010; date of current version September 22, 2010. The review of this paper was arranged by Editor S. Ringel.

A. Das, S. Ramanathan, and A. Rohatgi are with the School of Electrical and Computer Engineering, Georgia Institute of Technology (GIT), Atlanta, GA 30332-0250 USA (e-mail: arnab.das@gatech.edu).

V. Meemongkolkiat and D. S. Kim are with the Samsung Electronics Corporation Ltd., Gyeonggi-do 449-711, Korea.

Color versions of one or more of the figures in this paper are available online at http://ieeexplore.ieee.org.

Digital Object Identifier 10.1109/TED.2010.2057010

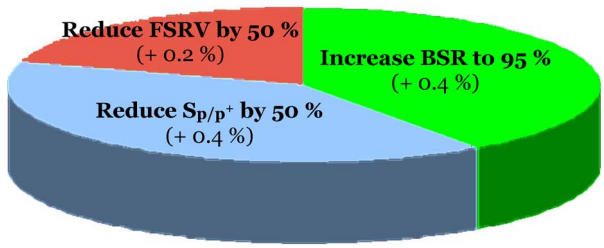

Fig. 1. PC1D modeling of the efficiency impact of improving the front and rear surfaces of a full Al-BSF solar cell.

II. PC1D Modeling of Advanced Cells

PC1D modeling shows that modifying the back side of a ~19% full Al-BSF cell has the largest impact on efficiency. Such a cell was fabricated and characterized and serves as the reference cell [1]. A PC1D fit to this 19% full Al-BSF cell reveals a back-surface recombination velocity (BSRV) of 600 cm/s, front-surface recombination velocity (FSRV) of 13 000 cm/s and a low internal back-surface reflectance (BSR) of 65%. Hereafter, the BSRV will be referred to as $S_{p/p}{}^+$ (the recombination velocity at the p/p^+ interface). Simulations (Fig. 1) show that backside improvements, namely, increasing BSR to 95% and reducing $S_{p/p}{}^+$ by 50%, would each contribute to 0.4% (abs.) increase in efficiency. In contrast, reducing the FSRV by 50% would add 0.2% to the efficiency. Additional modeling showed that the backside improvements alone can result in 20% cells if $S_{p/p}{}^+$ of 250 cm/s and BSR of 95% can be achieved.

Furthermore, the efficiency of a cell with improved rear parameters is also more tolerant of reductions in the substrate thickness (Fig. 2). PC1D modeling shows that the full Al-BSF cell would lose 1.2% (abs.) efficiency when the substrate thickness is reduced from 300 μm to 50 μm. The advanced 20% cell would lose just 0.6% (abs.) efficiency. It is also difficult to make full Al-BSF cells on such thin substrates without warping and if low-bow pastes are used, a penalty in BSF quality and V_{OC} is incurred [4], [5]. Hence, the modeled Al-BSF efficiencies in Fig. 2 should be taken as an upper bound.

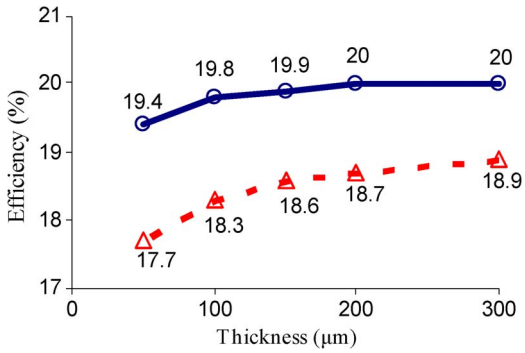

Fig. 2. PC1D modeling of the relationship between cell efficiency and substrate thickness for an 18.9% Al-BSF cell (dashed line) and an analogous cell (solid line) with improved BSRV (250 cm/s) and BSR (95%).

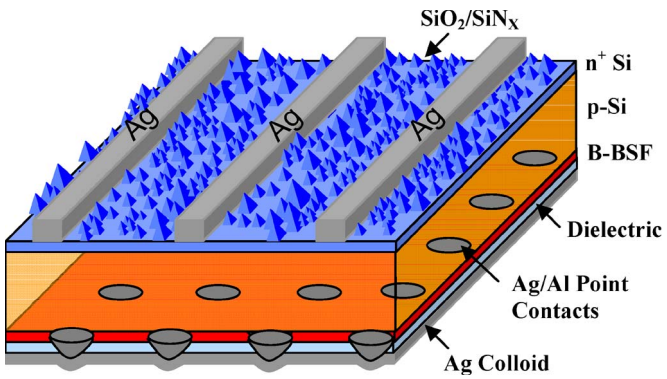

Fig. 3. Structure of B-BSF cell with rear dielectric passivation and SP contacts.

Since changing the backside of the Al-BSF structure has been identified as a promising route to higher efficiencies, alternative rear passivation schemes need to be explored. BSF formation via boron diffusion is a strong candidate since a p^+layer that is formed by boron diffusion can provide superior passivation due to a higher solid solubility limit in Si and does not cause bowing on thin substrates [6], [7]. However, boron diffusion is not common in industry, partly because it often results in contamination of the Si substrate [8]–[11]. Passivation of a heavily boron-doped silicon surface that remains stable through the contact firing step is a second challenge. This paper examines a novel SiO_2-based spin-on dielectric that performs both impurity gettering and surface passivation in a single thermal step. Tracking of the 'bulk' minority carrier lifetime through processing steps was used to quantify the gettering ability of the dielectric and compare its efficacy to that of $POCl_3$ gettering. Measurements of the interface charge density and surface passivation quality are used to determine the charge in the spin-on dielectric layer and its impact on surface passivation.

III. Experimental

SP n^+-p-p^+ solar cells with an active area of 4 cm^2 were fabricated on 1.3-Ω-cm 290-μm thick p-type float zone (FZ) Si (Fig. 3). It has previously been shown that dilute boric acid/deionized water solutions can be used for forming p^+ layers of a wide range of sheet resistances and that these layers can be passivated as well as those formed using more conventional sources such as BBr_3 [8]. To fabricate cells, random pyramid texturing was applied to the front side of the wafer. Subsequently, a full-area B-BSF was formed by spinning a 1-wt. % boric acid solution onto the backside of the wafer followed by tube furnace diffusion at 1000 °C for under 30 min to form a 40-Ω/□ p^+ layer. Next, $POCl_3$ diffusion was performed to form a 70-Ω/□ n^+ emitter (the boron-diffused rear was protected by a spin-on diffusion barrier during $POCl_3$ diffusion). Both the borosilicate and phosphosilicate glasses were then removed in a 5% HF/DI H_2O solution. In order to passivate the rear surface, the dielectric was spun onto the boron-doped rear and cured in O_2 ambient followed by a short anneal in an inert ambient, both at 900 °C. This step also results in a thin (∼15 nm) thermal oxide which passivates the emitter. After deposition of a plasma-enhanced chemical vapor SiN_X layer on the front, Ag and Ag/Al pastes were screen-printed on to the front (grid pattern) and rear (point contact pattern), respectively, and cofired. A thin conductive, light-scattering silver colloid film was used to electrically connect the rear point contacts and to serve as a back- surface reflector (BSR) [12]. A short 400 °C forming gas anneal was then performed to lower the contact resistance of the SP front contacts and to sinter the BSR layer.

The bulk minority carrier lifetime of samples after various processing steps was determined with the Transient-PCD method. Prior to measurement, all metals and dielectrics and ∼30 um of the Si surfaces were etched away and both surfaces were passivated with Iodine/Methanol solution. The quality of the dielectric-passivated boron-doped surfaces was quantified with saturation current density (J_0) and effective lifetime $(\tau_{\rm Eff})$ measurements using the Transient-PCD and QSS-PC methods, respectively [13], [14]. The J_0 and $\tau_{\rm Eff}$ samples were prepared on 500 Ω-cm n-type and 1.3 Ω-cm p-type FZ Si wafers, respectively, which were diffused with boron and passivated with the spin-on dielectric on both sides. From the measured bulk and effective lifetimes, the effective surface recombination velocity at the p/p^+ interface (S_{p/p^+}) was calculated using the relation

$$\frac{1}{\tau_{\rm Eff}} = \frac{1}{\tau_{\rm Bulk}} + \frac{2S_{p/p^+}}{L} \tag{1}$$

where L is the thickness of wafer being measured. The charge density and polarity of the dielectric were determined using undiffused 1.3-Ω-cm p-type FZ Si wafers which were passivated with the spin-on dielectric on both sides. The relevant information was then extracted from C–V measurements on these samples using a SemiTest SCA-2500 surface charge analyzer. Sheet resistances were determined by four-point probe measurements and doping profiles were obtained via secondary ion mass spectroscopy (SIMS).

IV. BSF Profiles of 20% Efficient Cells

The PC1D modeling of the advanced 20% cell in Fig. 2 was extended to incorporate a p^+ profile on the rear side to model a BSF. It was found that even with no surface passivation

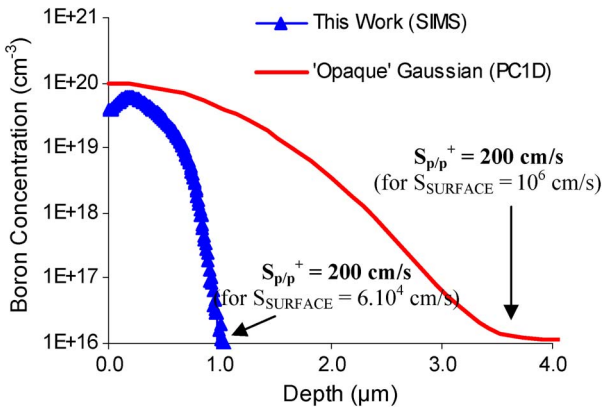

Fig. 4. Candidate B-BSF profiles and surface recombination velocities for 20% efficient SP cells.

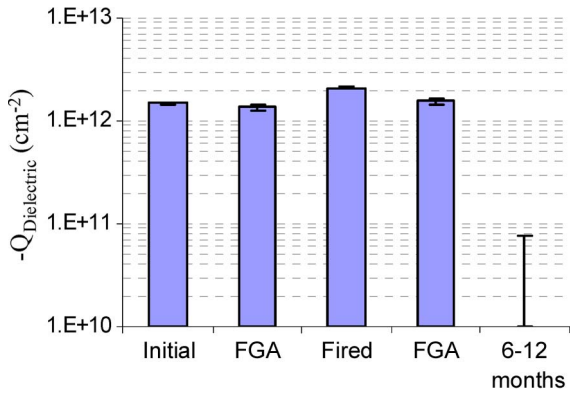

Fig. 5. Tracking of charge density in the spin-on dielectric through cell processing steps and over time.

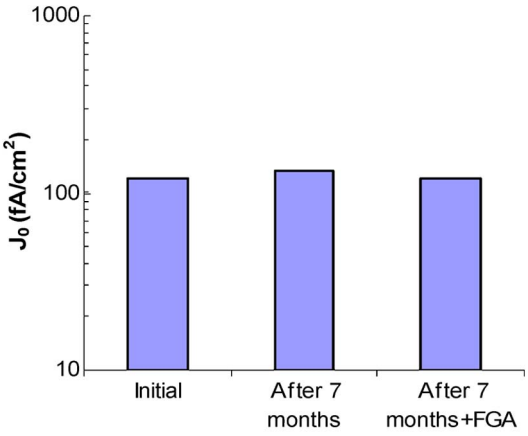

Fig. 6. Saturation current density of dielectric-passivated B-BSF over time.

($S = 10^6$ cm/s at the p^+ surface), a 3.5-μm deep, opaque B-BSF with surface concentration of 10^{20} cm^{-3} is sufficient for achieving 20% efficiency (Fig. 4). King and Swanson achieved a similar boron profile by using a 5-hr long process at 1000–1120 °C [15]. Since such a long, high-temperature processing step may be prohibitively expensive and slow for commercial cells, more lightly doped BSFs were explored in this paper. This work uses a 45-$\Omega/\square$ BSF layer which can be formed with a much shorter, lower temperature diffusion process as described earlier. Unfortunately, such shallow BSFs are electrically 'transparent' and with full-area rear metallization (i.e., no surface passivation), this 45-$\Omega/\square$ BSF would yield a S_{p/p^+} of 420 cm/s which is insufficient for achieving 20% efficiency. Modeling shows that in order to achieve the target S_{p/p^+} of $\leq$ 250 cm/s using this shallow BSF, an S at the metallized p^+ surface (hereafter referred to as $S_{SURFACE}$) of $\leq$ 60 000 cm/s is required. This requirement is currently not achievable using a full-area SP rear contact and therefore, process complexity in the form of an additional passivation step and local contacts is unavoidable. This increased complexity, relative to the full Al-BSF structure, is apparent in the cell structure shown in Fig. 3.

An additional, potential advantage of trading away process simplicity in exchange for a process with a lower thermal budget is higher bulk minority carrier lifetimes. Reduced bulk lifetimes in processes utilizing boron have been reported for numerous boron sources—the loss in lifetime can be traced to the generation of gliding misfit dislocations and the introduction of contaminant species with iron (Fe) being the most commonly suspected contaminant [16]–[18]. Both misfit dislocation generation and Fe contamination are more likely to occur with prolonged, high- temperature processes [19], [20].

Based on these considerations, the more complex process with a shallower B-BSF was chosen for this paper. Fig. 4 shows the SIMS profile of this BSF. The peak of the profile (6.10^{19} cm^{-3}) occurs 0.2 μm away from the surface due to outdiffusion of boron during the dielectric anneal step in oxygen that is part of the cell fabrication process [21].

V. Quality and Stability of Dielectric Passivation

The presence of negative charge density in a passivating dielectric is known to improve passivation of a p^+ layer due to the accumulation of holes at the dielectric/p^+ Si interface [22], [23]. The spin-on dielectric that was used in this paper has a negative charge density of ~1e12 cm^{-3} and after being passivated with this dielectric, the shallow B-BSF exhibits a J_{0e} of 122 fA/cm^2. Assuming a short-circuit current density, (J_{SC}) of 38 mA/cm^2 sets an open-circuit voltage (V_{OC}) limit of 690 mV. When the dielectric passivation was removed in HF, the J_{oe} increased to 715 fA/cm^2 which reduces the V_{oc} limit by more than 45 mV. Such a large increase in J_{oe} emphasizes the transparency of this shallow BSF.

Though the charge density ($Q_{Dielectric}$) in the spin-on dielectric is stable through the high-temperature contact firing step, it diminishes over a period of 6–12 months and some samples even exhibited a low ($< 10^{11}$ cm^{-2}) positive fixed-charge density similar to thermal SiO_2 (Fig. 5). This loss/reversal of charge in the spin-on dielectric may be expected to result in degradation of the passivation quality over time. However, the passivated B-BSF in this paper showed no such degradation. Both the saturation current density (J_0) and the implied V_{OC} (measured on the unmetallized cell structure in Fig. 1) remain stable over a period of 7–24 mo (Figs. 6 and 7). This indicates that the negative charge plays no appreciable role in passivating the B-BSF and that interface quality dictates the BSRV.

The apparent discrepancy between the results here and those in the literature stems from the fact that the effect of the dielectric charge on passivation depends on the following: 1) the

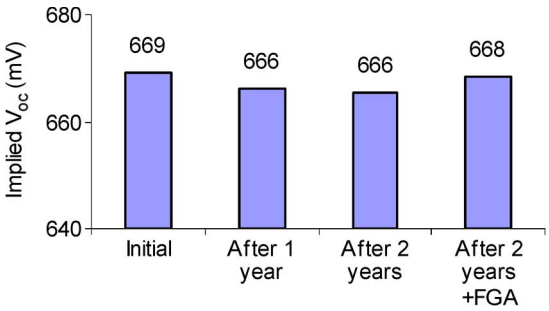

Fig. 7. Implied open-circuit voltage of unmetallized dielectric-passivated B-BSF solar cell over time.

magnitude of the charge; and 2) the surface/peak doping concentration. The relationship between passivation, charge density, and doping concentration was explored by further extending the PC1D modeling of the 20% cell in Fig. 2 by including a p^+ profile and a charge density at the p^+ surface. Change in the simulated cell V_{oc} was used as an indication of change in passivation quality. The results are summarized in Table I. For a BSF profile with a surface or peak boron concentration of 6.10^{19} cm^{-3}, a negative charge of -10^{12} cm^{-2} has a negligible effect (SIMS and Curve A profiles in Table I). This is in good agreement with the experimental implied V_{OC} results in Fig. 7. In general, the effect of a negative surface charge is higher for lower surface concentrations, and much larger for a charge density of $-1e13$ cm^{-2}. It is interesting to note that cells with a lower surface concentration BSF (Profiles B and C) start off with lower V_{OC} and efficiency; but with a surface charge density of $-1e13$ cm^{-2}, these cells outperform the high-surface-concentration BSF cells. Charge density of $-1e13$ cm^{-2} has been reported for atomic layer deposition Al_2O_3 films which implies that efficiencies beyond 20% may be possible with passivated shallow B-BSF cells [24]. While ohmic contacts have been made to such low-surface-concentration boron emitters using electroplated evaporated contacts, achieving the same with SP paste remains a challenge [22], [23]. The sheet resistances of profiles B and C in Fig. 8 are 200 and 270 Ω/sq, respectively.

It should be noted that the model used here deviates from reality in two ways. 1) Real boron profiles are not Gaussian [15], [21]. However, both the actual boron profile (Fig. 4—SIMS) and its Gaussian approximation (Fig. 8—Curve A) produce very similar results. 2) Though the profiles in Fig. 8 and Table I have different surface concentrations, the S at the p^+ surface was kept constant at 40 000 cm/s for all the profiles. This assumption was made in order to isolate the effect of charge alone on efficiency and was also experimentally reported by King *et al.* [15].

In order to be compatible with the SP method of forming contacts, passivating dielectrics also need to be stable through a high-temperature firing process. Fig. 9 shows that when subjected to a high-temperature firing cycle, the $S_{p/p}{}^+$ of the spin-on-dielectric-passivated B-BSF increased from 92 to 173 cm/s. Nevertheless, this is adequate for achieving high open-circuit voltages. Using PC1D, this increase in $S_{P/P}{}^+$ was found to be equivalent to V_{OC} loss of just 4 mV. A short forming gas anneal (FGA) at 400 °C restores $S_{p/p}{}^+$ to nearly the starting value. It should be noted that the Ag/Al paste used for making the rear point contacts readily fires through the dielectric and therefore, no opening of vias is required for making contacts to the B-BSF.

VI. Gettering Study

In order to translate good surface passivation to high efficiencies, a high minority carrier bulk lifetime is required. Historically, achieving high bulk lifetimes on boron-diffused Si has been more challenging than on phosphorus-diffused Si, particularly for cheaper boron sources such as spin-on and paste dopants [8]–[11]. Fig. 10 shows that immediately after boron diffusion using boric acid, the average bulk lifetime drops by $\sim$80%. After a subsequent $POCl_3$ diffusion to form the solar cell emitter, the lifetime recovers, but only to 40% its initial value. It is only during the final surface passivation step in which the negatively charged dielectric layer is spun onto the boron-doped rear and annealed at 900 °C that the bulk lifetime completely recovers. It should be noted that this same dielectric is used to block $POCl_3$ diffusion into the B-BSF. However, it was found that under the $POCl_3$ diffusion conditions (a mixture of $N_2/O_2/POCl_3$ ambient at 860 °C), the dielectric does not contribute to gettering. In order to isolate the relative impact of the two gettering steps in the cell fabrication process, boron-diffused samples were subjected to $POCl_3$-only gettering and dielectric-only gettering. Fig. 11 shows that dielectric gettering alone is sufficient to completely restore the bulk lifetime of the boron-diffused silicon substrate. It should be noted that the dielectric-only gettered samples were subjected to the thermal cycle of $POCl_3$ diffusion in order to mimic the cell fabrication process; however, no $POCl_3$ diffusion was performed so the bulk lifetime recovery is attributed entirely to gettering by the dielectric.

These results indicate that, when appropriately annealed, gettering by the dielectric is more effective than $POCl_3$ gettering. This unexpected result may be caused by contaminants being concentrated in or near the boron-diffused rear surface. Since $POCl_3$ diffusion occurs from the front side of the substrate, the contaminants may be too far away to be effectively gettered during $POCl_3$ diffusion. This theory was confirmed by subjecting rear-side boron-diffused wafers to either front-side dielectric gettering or rear-side dielectric gettering (Fig. 12). The bulk lifetime after front-side gettering is only 60% of the lifetime achieved by rear-side gettering. This confirms that impurities introduced by the boron diffusion are not uniformly distributed within the wafer but are concentrated within and/or near the p^+ layer. In a separate study, the quasi-steady-state photoconductivity method was used to determine that the contaminant responsible for the loss of bulk lifetime is iron [25]. The composition of the dielectric and its iron-gettering mechanism are currently under study.

VII. Advanced Solar Cell Characterization

Using the process sequence described earlier, 20% efficient dielectric-passivated B-BSF cells (4 cm^2) were achieved on 1.3-Ω-cm FZ Si. The National Renewable Energy Laboratory

TABLE I
PC1D MODELING SHOWING THAT THE EFFECT OF REAR-DIELECTRIC CHARGE DEPENDS ON THE BSF DOPING PROFILE

B-BSF Profile	Initial Cell V_{OC} (mV)	ΔV_{OC} due to dielectric charge density		Initial Cell Efficiency (%)	Efficiency after applying dielectric charge density	
		$Q_{Dielectric} = -10^{12}$ cm^{-2}	$Q_{Dielectric} = -10^{13}$ cm^{-2}		$Q_{Dielectric} = -10^{12}$ cm^{-2}	$Q_{Dielectric} = -10^{13}$ cm^{-2}
SIMS (Fig. 4)	648	+ 2 mV	+ 6 mV	20	20.1 %	20.4 %
A (Fig. 8)	649	+ 2 mV	+ 7 mV	20.1	20.2 %	20.5 %
B (Fig. 8)	644	+ 6 mV	+ 16 mV	19.8	20.2 %	20.7 %
C (Fig. 8)	641	+ 8 mV	+ 19 mV	19.7	20.1 %	20.7 %

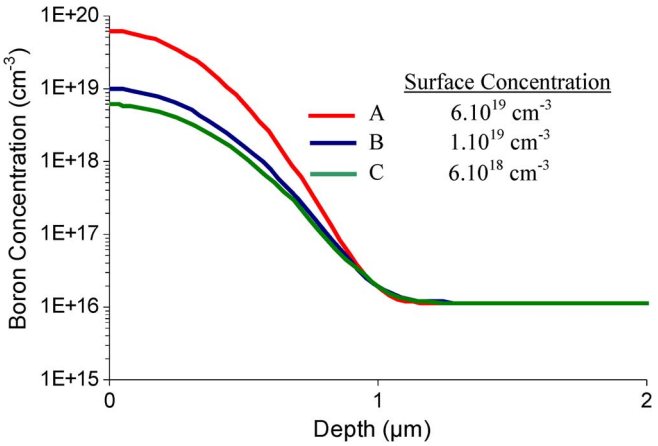

Fig. 8. B-BSF profiles used for PC1D simulation study into the effect the dielectric charge on cell efficiency.

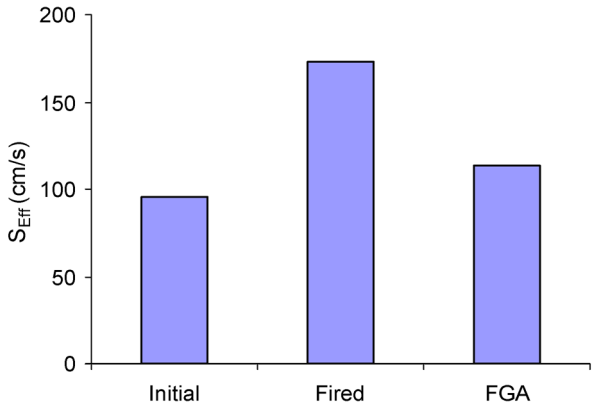

Fig. 9. Change in surface recombination velocity of unmetallized dielectric-passivated B-BSF due to contact firing process.

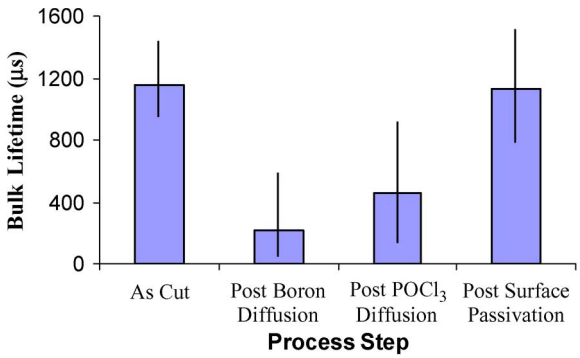

Fig. 10. Bulk minority carrier lifetime of 1.3-Ω-cm FZ Si wafers at various stages of solar cell processing.

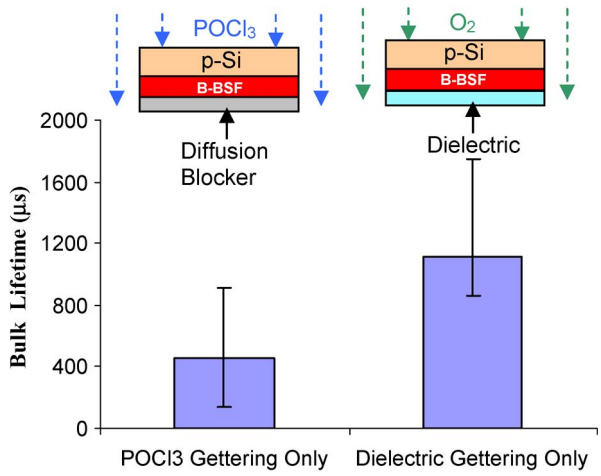

Fig. 11. Bulk minority carrier lifetime of boron-diffused wafers after $POCl_3$ gettering and dielectric gettering. The insets show the structure of the samples for each gettering process.

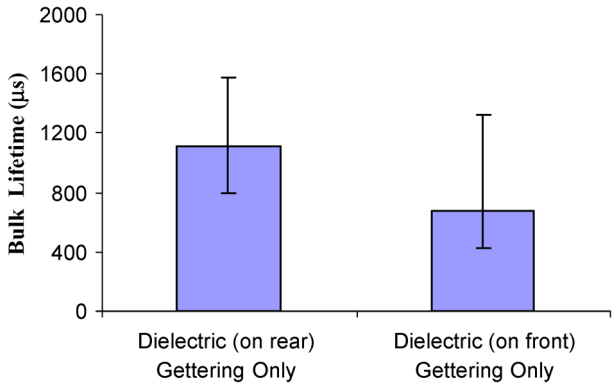

Fig. 12. Effect of side of wafer from which gettering is performed on bulk minority carrier lifetime. All samples have a boron-doped rear surface and an undiffused front surface.

(NREL) measured I–V characteristics of one such cell is shown in Fig. 13. This cell was measured at NREL 1–8 months after being fabricated and the difference in efficiency between the two measurements was just 0.03%. (abs.) This provides further evidence that the B-BSF used in this paper is insensitive to the negative dielectric charge which was found to disappear over this time period.

A PC1D fit (Fig. 14) made to the IQE and IV characteristics of the cell was used to extract a S_{p/p^+} value of 210 cm/s, a $S_{SURFACE}$ of 45 000 cm/s, and a BSR of 95%. This confirms the accuracy of our PC1D modeling which had predicted that S_{p/p^+} of 250 cm/s, $S_{SURFACE}$ of 60 000 cm/s, and a BSR of

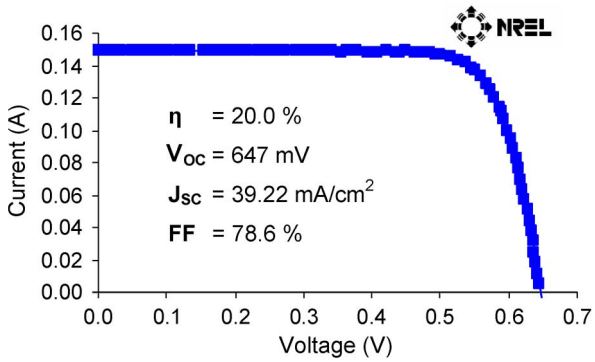

Fig. 13. I–V characteristic of an SP dielectric-passivated B-BSF solar cell.

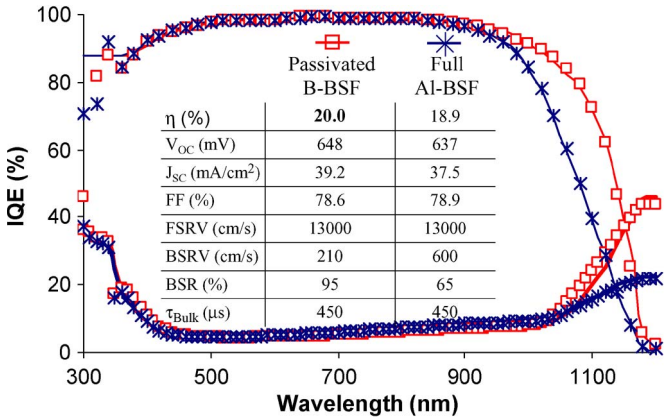

Fig. 14. PC1D fits (solid lines) to the measured IQE curves (open points) of a 20% dielectric-passivated B-BSF cell and an 18.9% full Al-BSF cell. The inset shows the PC1D I–V output and selected PC1D input parameters.

95% are required to achieve 20% efficient cells. Fig. 14 also shows the IQE curve and corresponding cell parameters for the analogously processed 18.9% (NREL-verified) full Al-BSF cell that was used as the baseline cell for PC1D modeling. The improved BSR and BSRV values of the dielectric-passivated B-BSF cell are each responsible for an efficiency increase of ~0.5%. The bulk lifetime of 450 μs for both cells is a significant drop from the premetallization lifetime of ~1 ms and may be caused by the diffusion of impurities into the substrate during contact firing. However, the corresponding diffusion length of ~1100 μm is sufficient for complete carrier collection.

Long wavelength light-beam-induced current (LBIC) maps confirm that the shallow B-BSF in this paper is electrically transparent as expected (Fig. 15). The SP screen-printed dots on the rear side are visible as regions of degraded passivation. From the measured dimensions of the degraded spots, the S_{p/p^+} under the dielectric (114 cm/s - Fig. 9) and the extracted effective S_{p/p^+} of the cell (210 cm/s - Fig. 14), the S_{p/p^+} under the metal point contacts was calculated to be ~950 cm/s. This indicates that the transparent B-BSF is partially successful at decoupling the p/p$^+$ interface from the p$^+$/SP metal surface. Without this decoupling, the S_{p/p^+} under the point contacts would have been ~10^6 cm/s, resulting in a effective S_{p/p^+} of 15 000 cm/s which would be too high to achieve 20% efficient cells.

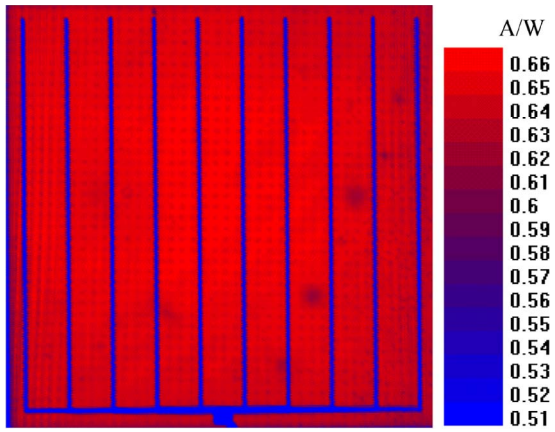

Fig. 15. 980-nm LBIC map of dielectric-passivated B-BSF solar cell showing spots of degraded passivation under the rear SP point contacts.

VIII. Conclusion

A 20% efficient B-BSF solar cell with SP contacts has been presented. Modeling has been used to find multiple routes to achieve 20% efficient BSF cells, each with their strengths (in terms of process simplicity and maximum achievable efficiency) and weaknesses (in terms of process complexity, thermal budget, and ease of contacting). The approach used here involves a low thermal budget, screen-printing-friendly process which requires surface passivation of the B-BSF to achieve high efficiencies. The spin-on dielectric introduced in this paper serves as both the passivating layer and as an effective Fe-gettering site which allows it to reverse the bulk lifetime degradation that is common in boron diffusions. Both functions are performed in a single thermal step. Gettering studies have demonstrated that the gettering ability of the dielectric is similar to that of $POCl_3$ gettering and that having the gettering site close to the boron doped layer is important for achieving complete recovery of the bulk lifetime. Since the dielectric is applied to the boron-doped side, it offers a superior gettering solution compared to $POCl_3$. Experimental and modeling passivation studies showed that a negative charge density of $-1e12$ cm^{-2} does not significantly contribute to passivation of the very heavily doped p$^+$ surfaces used in this paper. Instead, the quality of the interface between the spin-on dielectric and p$^+$ Si is responsible for the low surface recombination velocity (S_{p/p^+}) of 92 cm/s that was achieved.

Acknowledgment

The authors would like to thank R. Reedy and P. Ciszek, both at the National Renewable Energy Laboratory (NREL) for performing SIMS measurements and I–V measurements, respectively.

References

[1] A. Rohatgi, A. Ristow, A. Das, and S. Ramanathan, "Road to cost effective silicon PV," in *Proc. Tech. Dig. 18th Int. PVSEC, IACS*, Kolkata, India, Jan. 2009.

[2] A. Das, V. Meemongkolkiat, D. S. Kim, S. Ramanathan, and A. Rohatgi, "20% Efficient screen printed boron BSF cells using spin-on dielectric passivation," in *Proc. 34th IEEE PVSC*, Jun. 2009, pp. 000477–000481.

[3] P. A. Basore, "Numerical modeling of textured silicon solar cells using PC-1D," *IEEE Trans. Electron Devices*, vol. 37, no. 2, pp. 337–343, Feb. 1990.
[4] N. Merchant, A. Shaik, C. Khadilkar, S. Sridharan, and E. Graddy, "SEM microstructure, composition, property correlation-ships in aluminum conductors," in *Proc. 33rd IEEE PVSC*, May 2008, pp. 1–3.
[5] A. Ebong, K. Nakayashiki, V. Upadhyaya, A. Rohatgi, B. R. Bathey, M. D. Rosenblum, J. Salami, and A. Shaikh, "Screen-printed solar cells on less than 200-μm thick EFG sheet silicon," in *Proc. 22nd EU-PVSEC*, Sep. 2007, pp. 1442–1445.
[6] G. L. Vick and K. M. Whittle, "Solid solubility and diffusion coefficients of boron in silicon," *J. Electrochem. Soc.*, vol. 116, no. 8, pp. 1142–1144, Aug. 1969.
[7] F. A. Trumbore, "Solid solubilities of impurity elements in germanium and silicon," *Bell Syst. Tech. J.*, vol. 39, no. 1, pp. 205–233, Jan. 1960.
[8] A. Das, D. S. Kim, K. Nakayashiki, B. Rounsaville, V. Meemongkolkiat, and A. Rohatgi, "Boron Diffusion with boric acid for high efficiency silicon solar cells," *J. Electrochem. Soc.*, pp. H684–H687, May 2010.
[9] G. Bueno, I. Freire, K. Varner, L. Pérez, R. Lago, J. C. Jimeno, J. Salami, H. Kerp, K. Albertsen, and A. Shaikh, "Simultaneous diffusion of screen printed boron and phosphorous paste for bifacial silicon solar cells," in *Proc. 20th EU-PVSEC*, Jun. 2005, pp. 1458–1461.
[10] R. Meyer, P. Engelhart, B. Terheiden, and R. Brendel, "A process sequence for silicon solar cells with local boron back surface field," in *Proc. 21st EU-PVSEC*, Sep. 2006, pp. 713–716.
[11] Y. Komatsu, V. D. Mihailetchi, L. J. Geerligs, B. van Dijk, J. B. Rem, and M. Harris, "Homogeneous p+ emitter diffused using boron tribromide for record 16.4% screen-printed large area n-type mc-Si solar cell," *Sol. Energy Mater. Sol. Cells*, vol. 93, no. 6, pp. 750–752, 2009.
[12] A. Das and A. Rohatgi, "Optical and electrical characterization of silver microflake colloid films," *J. Electrochem. Soc.*, vol. 157, no. 3, pp. H301–303, Jan. 2010.
[13] D. E. Kane and R. M. Swanson, "Measurement of the emitter saturation current by a contactless photoconductivity decay method," in *Proc. 18th IEEE PVSC*, 1985, pp. 578–583.
[14] R. Sinton and A. Cuevas, "Contactless determination of current-voltage characteristics and minority-carrier lifetimes in semiconductors from quasi-steady state photoconductance data," *Appl. Phys. Lett.*, vol. 69, no. 17, pp. 2510–2512, Oct. 1996.
[15] R. R. King and R. M. Swanson, "Studies of diffused boron emitters: Saturation current, bandgap narrowing, and surface recombination velocity," *IEEE Trans. Electron Devices*, vol. 38, no. 6, pp. 1399–1409, Jun. 1991.
[16] P. J. Cousins and J. E. Cotter, "The influence of diffusion-induced dislocations on high efficiency silicon solar cells," *IEEE Trans. Electron Devices*, vol. 53, no. 3, pp. 457–464, Mar. 2006.
[17] X. J. Ning, "Disolocations induced by boron diffusion in silicon: A transmission electron microscopy study," *Philos. Mag. A, Phys. Condens. Matter Defects Mech. Prop.*, vol. 75, no. 1, pp. 115–135, Jan. 1997.
[18] N. Ohe, K. Tsutsui, T. Warabisako, and T. Saitoh, "Effect of boron gettering on minority-carrier quality for FZ and CZ Si substrates," *Sol. Energy Mater. Sol. Cells*, vol. 48, no. 1–4, pp. 145–150, Nov. 1997.
[19] F. Gaiseanu, G. Kissigner, D. Kruger, and H. Richter, "Analysis of the generation of the Misfit dislocations during the boron prediffusion in silicon," *Proc. SPIE*, vol. 3507, pp. 281–289, Sep. 1998.
[20] A. A. Istratov, H. Hieslmair, and E. R. Weber, "Iron and its complexes in silicon," *Appl. Phys. A, Solids Surf.*, vol. 69, no. 1, pp. 13–44, May 1999.
[21] S. M. Sze, *Semiconductor Devices: Physics and Technology*. Murray Hill, NJ: AT&T Bell Lab., 1985.
[22] J. Benick, H. Hieslmair, and E. R. Weber, "Comprehensive studies of passivation quality on boron diffused silicon surfaces," in *Proc. 22nd EU-PVSEC*, Sep. 2007, pp. 1244–1247.
[23] J. Benick, B. Hoex, M. C. M. van de Sanden, W. M. M. Kessels, O. Schultz, and S. W. Glunz, "High efficiency n-type Si solar cells on Al2O3-passivated boron emitters," *Appl. Phys. Lett.*, vol. 92, no. 25, p. 253504, Jun. 2008.
[24] G. Agostinelli, A. Delabie, P. Vitanov, Z. Alexieva, H. F. W. Dekkers, S. De Wolf, and G. Beaucarne, "Very low surface recombination velocities on p-type silicon wafers passivated with a dielectric with fixed negative charge," *Sol. Energy Mater. Sol. Cells*, vol. 90, no. 18/19, pp. 3438–3443, Nov. 2006.
[25] D. H. Macdonald, L. J. Geerligs, and A. Azzizi, "Iron detection in crystalline silicon by carrier lifetime measurements for arbitrary injection and doping," *J. Appl. Phys.*, vol. 95, no. 3, pp. 1021–1028, Feb. 2004.

Arnab Das received the B.S. degree in computer engineering from Georgia Institute of Technology (GIT), Atlanta, in 2004.

He then joined the University Center of Excellence for Photovoltaics at GIT where he is currently working toward the Ph.D. degree in Electrical Engineering. His current research interests include the fabrication and characterization of silicon photovoltaic devices with emphasis on surface passivation and optical trapping.

Vichai Meemongkolkiat was born in Bangkok, Thailand, in 1980. He received the Bachelor's of Engineering degree in electrical engineering from the Chulalongkorn University, Bangkok, Thailand, in 2001. He received the Master's of Science degree and Doctorate of Philosophy in the school of electrical and computer engineering from Georgia Institute of Technology (GIT), Atlanta, in 2007 and 2008, respectively.

He is currently a Senior Engineer at Samsung Electronics in South Korea. His primary research interest is in crystalline silicon solar cells.

Dong Seop Kim received the B.S. degree in metallurgical engineering from Seoul National University, Seoul, Korea, in 1988, and the M.S. and Ph.D. degrees in material science from Korea Advanced Institute of Technology, Daejeon, Korea, in 1990 and 1994, respectively.

His doctoral research was focused on fabrication and analysis of CdTe solar cells. In 1994, he joined the photovoltaic laboratory at the Samsung Advanced Institute of Technology, Yongin, Korea, where he worked on the development of high-efficiency crystalline silicon solar cell for 5 years and on polycrystalline thin-film transistors for 2 years. In 1998, he was a Postdoctoral Fellow in material science at University of Illinois, Urbana- Champaign, where he studied deposition of polycrystalline silicon on glass substrate for thin-film transistors and solar cells. In 2001, he joined the University Center of Excellence for Photovoltaics Research and Education (UCEP), Georgia Institute of Technology (GIT), Atlanta, to study low-cost high-efficiency manufacturable Si solar cells as an Assistant Director for 5 years. He has taught mathematics, electromagnetic, semiconductor devices, and electronic circuit as an Assistant Professor in the Electronic Engineering at Sejong University in South Korea. Currently, he is working at Samsung Electronics as a Vice President for Research and Development of solar cells. His current research interests are modeling, fabrication, and characterization of high-efficiency Si and compound semiconductor solar cells; development of new processes applicable to mass production; and surface and bulk passivation.

Dr. Kim received Samsung Technology Award and Best Paper Award at Samsung Corporation for outstanding achievement in developing high-efficiency silicon solar cells. He also received several best paper awards at international photovoltaic conferences.

Saptharishi Ramanathan was born in Chennai, India, in 1980. He received the Bachelor of Technology in metallurgical engineering from Indian Institute of Technology Madras (IIT M), Chennai, India, in 2002. He received the Master of Science degree in engineering science from Pennsylvania State University, University Park, in 2004.

He is currently working toward the Ph.D. degree in School of Electrical and Computer Engineering at Georgia Institute of Technology (GIT), Atlanta. His research interests include the fabrication of high-efficiency crystalline silicon solar cells.

Ajeet Rohatgi (F'91) received the B.S. degree in electrical engineering from the Indian Institute of Technology, Kanpur, India, in 1971, the M.S. degree in materials engineering from Virginia Polytechnic Institute and State University, Blacksburg, in 1973, and the Ph.D. degree in metallurgy and material science from Lehigh University, Bethlehem, PA, in 1977.

He is a Regents' Professor and a Georgia Power Distinguished Professor in the School of Electrical Engineering. He is the Founding Director of the University Center of Excellence for Photovoltaic Research and Education at Georgia Institute of Technology, Atlanta, and the Founder and CTO of Suniva Inc. Before joining the Electrical Engineering faculty at GIT in 1985, he was a Westinghouse Fellow at the Research and Development Center, Pittsburgh, PA. His current research interests include development of cost and efficiency roadmaps for attaining grid parity with Silicon PV, understanding of impurity effects in silicon solar cells, gettering and passivation of defects in solar grade silicon, rapid thermal processing of solar cells, design and fabrication of low-cost high-efficiency cells on mono and multicrystalline silicon, and design, performance and economics of photovoltaic systems.

Dr. Rohatgi has published over three hundred and seventy technical papers in this field and has been awarded 11 patents. He is on the editorial board of several PV publications and served as General Chair for the 28th IEEE Photovoltaic Specialists Conference in Alaska in 2000. Dr. Rohatgi received the Westinghouse Engineering Achievement Award in 1985 and the Georgia Tech Distinguished Professor Award in 1996 for his research on high-efficiency solar cells. In 2003, he received the IEEE PVSC William Cherry Award and the NREL/DOE Rappaport Award for his contributions to Photovoltaics. In 2007, he received the Georgia Institute of Technology Outstanding Research Program Development Award. In 2008, he was recognized as one of the five most influential people in renewable energy by Power Finance & Risk Magazine and also by Georgia Sierra club for his efforts to help move both GA. and the U.S. into a clean energy economy through his solar energy research at GT. In 2009, he received the Envention Award for conservation and pollution-curbing efforts by the Atlanta Business Chronicle, the Climate Protection Award for dedication and technical innovation in photovoltaics by the EPA, and the Hoyt Clark Hottel Award for outstanding educator and innovator in the field of photovoltaics by the American Solar Energy Society.